Conformational Polymorphism of Amphiphilic Polymers in a Poor Solvent

Valentina V. Vasilevskaya,[†] Pavel G. Khalatur,*[,‡] and Alexei R. Khokhlov[‡,§]

Nesmeyanov Institute of Organoelement Compounds, Russian Academy of Sciences, Moscow 117823, Russia; Department of Polymer Science, University of Ulm, Ulm D-89069, Germany; and Physics Department, Moscow State University, Moscow 119899, Russia

Received July 22, 2003; Revised Manuscript Received October 14, 2003

ABSTRACT: To simulate amphiphilic polymers, we introduce an extended hydrophobic/hydrophilic (HP) model which, in contrast to the standard "beads-on-a-string" HP model, incorporates the dualistic nature of monomer units, each consisting of hydrophobic (H) and hydrophilic (P) interaction sites. For this coarse-grained model, the hydrophobically driven conformational transitions are studied using extensive molecular dynamics simulations. We find that, depending on the interaction between H and P sites, a variety of thermodynamically stable anisometric chain morphologies are possible in a solvent selectively poor for H sites, including disklike structures, stretched strings of intramolecular micelles, and cylindrical-shaped conformations. These microstructures are formed due to intramolecular segregation of chemically different H and P groups. Under certain conditions, the chain size R_g as a function of solvent quality can behave in a nonmonotonic manner, showing an increase when the solvent becomes poorer for hydrophobic sites. For the range of the chain lengths N simulated ($N \leq 1024$), the formation of highly anisotropic conformations can lead to the $R_g \propto N^{0.9}$ scaling.

Introduction

Amphiphilic polymers contain both hydrophilic and hydrophobic groups, which have different affinity to water or other polar solvents. Some examples of synthetic polymers with amphiphilic properties of a monomer unit are poly(1-vinylimidazole), poly(*N*-isopropylacrylamide), and poly(2-ethylacrylic acid); they are shown in Figure 1. Also, many of the important biopolymers (proteins, polysaccharides, phospholipids, etc.) are typical polyamphiphiles. Moreover, among the synthetic polymers, polyamphiphiles are very close to biological macromolecules in nature and behavior. In principle, they may provide useful analogues of proteins and are important for modeling some fundamental properties and sophisticated functions of biopolymers such as protein folding and enzymatic activity. Since amphiphilic polymers contain both hydrophobic and hydrophilic groups, they can exhibit conformational transitions induced by temperature, solvent composition, or pH variation. In particular, the hydrophobicity of amino acids is assumed to be the main driving force for the formation of a unique (native) protein conformation.

The simplest model of hydrophobic/hydrophilic polymers is the so-called HP model introduced by Lau and Dill.[1,2] This two-letter (or "black-and-white") model, widely used in theoretical studies, involves only two types of monomer units, H (hydrophobic) and P (hydrophilic or polar), and reflects the spirit of minimalist models, in that it is simple yet based on a physical principle. With this model, an amphiphilic polymer is considered as a chain in which H and P groups are assumed to be pointlike interaction sites distributed along the chain in a linear fashion. It is assumed that, in water and other polar solvents, the hydrophilic groups are in a good solvent, while hydrophobic groups are in a poor solvent, so that they tend to aggregate.

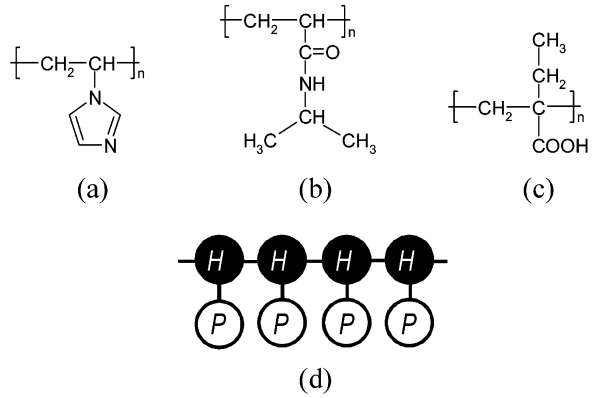

Figure 1. Examples of amphiphilic polymers: (a) poly(1-vinylimidazole), (b) poly(*N*-isopropylacrylamide), (c) poly(2-ethylacrylic acid), and (d) the HP side-chain model of an amphiphilic homopolymer.

Phenomenologically, hydrophobicity can be described as a tendency of hydrophobic polymer groups to reduce as much as possible their surface of contact with a polar solvent: two hydrophobic groups try to stick together in order to hide from polar solvent their mutual surface of contact. Consequently, hydrophobicity is introduced in the HP model as an effective (solvent-mediated) attraction between H monomer units. On the other hand, the hydrophilic (polar) groups tend to be surrounded by solvent molecules so that the solvent-mediated interaction between these groups is effectively repulsive. They also show a tendency to segregate from hydrophobic polymer segments. Such simple models can be studied using both computer simulations and approximate mean-field theoretical methods. What makes these models so interesting is the competition of the hydrophobic−hydrophilic effects.

The behavior of lattice and continuous (off-lattice) HP models, which neglect atomic detail for computational

[†] Russian Academy of Sciences.
[‡] University of Ulm.
[§] Moscow State University.
* Corresponding author. E-mail: Khalatur@germany.ru.

10.1021/ma0350563 CCC: $25.00
Published on Web 11/25/2003

tractability, has been the subject of an extensive research for many recent years, including the theoretical studies of collapse transition under various solvent conditions as well as protein folding.[3−11] With this coarse-grained model, a high temperature T corresponds to a good solvent condition, where the excluded-volume interactions dominate the attractions between nonbonded hydrophobic groups, and as a result, the flexible HP polymer is swollen. Thus, its radius of gyration, R_g, scales as $R_g \propto N^{\nu}$, where N is the chain length and $\nu \approx 0.59$ in three-dimensional (3d) space. However, as the solvent conditions worsen (i.e., T is decreased), the attractions between monomers become more effective, and under certain conditions, corresponding to the Flory Θ point (or the Θ temperature), they cancel to a large extent the excluded-volume interactions and the intrachain hydrophilic repulsions, and the 3d chain behaves in many respects like a Gaussian chain with $\nu = 1/2$. In yet poorer solvents (or at yet lower temperatures), the hydrophobic attractions prevail and the chain can collapse, forming a compact globular conformation which is of minimal surface-to-volume ratio, i.e., $\nu = 1/3$. In this state, the HP copolymer has a central spherical core formed by the hydrophobic groups that push outside the polar units. The latter form an outside corona that tends to be as far as possible from the hydrophobic core, though subject to the molecular connectivity. Theoretically, it was shown that the coil-to-globule transition in the flexible-chain polymer is a smooth second-order phase transition, while it is a sharp first-order phase transition in the case of semiflexible and rigid chains.[12,13] Also, it is known that the structure of arising globule itself depends on the local chain conformation and the distribution of attracting monomers along the chain. In particular, flexible homopolymer chains collapse into a spherical globular core while semiflexible chains can form compact toroidal structures. However, despite the difference in coil-to-globule transitions and the structure of arising globules, the radius of gyration is expected to be proportional to $N^{1/3}$.[13]

The standard "beads-on-a-string" HP model[1,2] is very simple and computationally efficient, but its principal disadvantage is the representation of each monomer unit of an amphiphilic chain as a pointlike interaction site of pure hydrophilic or pure hydrophobic type. At the same time, it is well-known that in the large majority of real amphiphilic polymers each monomer unit has a dualistic (hydrophobic/hydrophilic) character, that is, repeating polymer unit, which is considered as hydrophilic but actually incorporates both hydrophilic and hydrophobic parts concurrently. A typical example is poly(1-vinylimidazole) with the hydrocarbon (hydrophobic) backbone and hydrophilic water-soluble side groups (see Figure 1). Many of amino acids also contain both hydrophilic and hydrophobic groups simultaneously, and strictly speaking, the interaction between such amino acid residues in proteins cannot be literally reduced to pure hydrophilic or pure hydrophobic site−site interactions, as it is presupposed in the HP model.[1,2]

One of the possible extensions of the HP model is that we will call the HP side-chain model. This is a more realistic model of amphiphilic polymers where the dualistic character of each monomer unit is explicitly represented. In terms of graph theory, an amphiphilic polymer is modeled as a caterpillar graph instead of a linear graph corresponding to the standard HP model. More formally, a caterpillar of length N is the **HP** graph in which the set $\{\mathbf{H} = H_1, ..., H_N\}$ represents the nodes in the backbone and the set $\{\mathbf{P} = P_1, ..., P_N\}$ the so-called legs. Each backbone node corresponds to a hydrophobic group (e.g., CH_2−CH group in Figure 1), whereas the leg is considered as a polar side group attached to the node with the same number.

As we will see in this paper, such a trivial modification of the standard HP model can lead to some nontrivial consequences when studying the collapse for the single-chain amphiphilic polymer. Specifically, our aim here is to report the results of molecular dynamics simulations of the hydrophobically driven conformational transitions in the HP side-chain model under the variation of solvent conditions as well as to get an insight into the equilibrium structure of arising conformations. We will show that for this model a variety of novel structures with high complexity, including extended anisometric structures with cylindrical symmetries, are possible under poor solvent conditions for hydrophobic groups.

Methodology

A schematic representation of the model used in our study is shown in Figure 1. In the numerical simulations, we employ a continuum space (bead−rod) model, as opposed to widely used lattice HP models,[1,2] since the latter have intrinsically discretized dynamics of a rather arbitrary nature and have slow relaxation for a dense globular state. The time evolution of the system is determined by Newton's equations that are solved by using the method of molecular dynamics (MD).[14] Each monomer unit is modeled by a "dumbbell" consisting of H and P beads linked by rigid bonds of a fixed length. The dumbbells form an HP polymer with the backbone of N hydrophobic beads connected in a linear fashion and N hydrophilic beads attached to the backbone, as shown in Figure 1. In MD simulations, the bonds within a given macromolecule are constrained to length $b = 1.0$ using the RATTLE algorithm.[15]

The HP polymer contains $2N$ ($= N_H + N_P$) beads interacting through classical short-range van der Waals forces. Excluded volume between any nonbonded beads is included via a repulsive soft-core Lennard-Jones potential

$$u_{ev}(r_{ij}) = \begin{cases} 4\epsilon\left[\left(\frac{\sigma}{r_{ij}}\right)^{12} - \left(\frac{\sigma}{r_{ij}}\right)^{6} + \frac{1}{4}\right], & r_{ij} \le r_0 \\ 0, & r_{ij} > r_0 \end{cases} \quad (1)$$

where r_{ij} is the distance between the interaction sites i and j, $\sigma = \epsilon = 1$, and $r_0 = 2^{1/6}\sigma$ is a cutoff distance. The normalized parameter ϵ entering this equation controls the energy scale, whereas σ determines the length scale.

In addition to the excluded-volume potential (1), the nonbonded beads interact via a Yukawa-type potential, for which we use the following form:[11]

$$u_s(r_{ij}) = \frac{\epsilon_{\alpha\beta}\sigma}{r_{ij}} f(r_{ij}, r_c) h(r_c - r_{ij}) \quad (2)$$

Here, $f(r_{ij}, r_c) = [1 - (r_{ij}/r_c)]^2$ is the screening function, $h(r)$ is the Heaviside function, the parameter $\epsilon_{\alpha\beta}$ ($= \epsilon_{HH}$, ϵ_{PP}, ϵ_{HP}) sets the amplitude of the nonlocal site−site interactions, and $r_c = 4\sigma$ is the screening length, i.e., the cutoff distance for these interactions. In the model, this potential describes the solvent-mediated short-range hydrophobic−hydrophilic intrachain interactions.

The characteristic energies of H−H, H−P, and P−P interactions are considered to be variable parameters (all the energies are measured in units of ϵ). For $\epsilon_{\alpha\beta} = 0$, there is no additional repulsion (attraction) between chain beads except that corresponding to the excluded volume potential (1). The nature of hydrophobic forces is complicated,[16−18] but for the purpose of the present study it is sufficient to introduce a nonspecific short-range attraction using potential (2) in which the (negative) parameter ϵ_{HH} is chosen to promote the collapse of the chains. Note that in the strong segregation regime[19] the effective energy of attraction between hydrophobic groups must be, by definition, much larger than k_BT ($\sim 10k_BT$).[20] For simplicity, we assume that the solvent molecules surrounding the chain are identical to the hydrophilic beads so that $\epsilon_{PP} = 0$. The nonzero (positive) parameter ϵ_{HP} characterizes the H−P repulsion and promotes the intrachain segregation of H and P beads.

As an integral measure of solvent quality, it is instructive to define the following partial bare second virial coefficients

$$v_{\alpha\beta}^{(2)}(\epsilon_{\alpha\beta}) = 2\pi\int_0^{r_c}\{1 - \exp[-u_{\alpha\beta}(r)/k_BT]\}r^2\,dr \quad (3)$$

where $u_{\alpha\beta}(r) = u_{ev}(r) + u_s(r)$ and α, β = H, P. Using $v_{\alpha\beta}^{(2)}(\epsilon_{\alpha\beta})$, we define the normalized values $v_{\alpha\beta} = {}^1/_4 v_{\alpha\beta}^{(2)}(\epsilon_{\alpha\beta})/v_{\alpha\beta}^{(2)}(0)$ and then introduce the linear combination

$$v = v_{HH} + v_{PP} + 2v_{HP} \quad (4)$$

The parameter v is similar to the excluded-volume parameter ${}^1/_2 - \chi$, where χ is the Flory−Huggins interaction parameter, and characterizes solvent quality in an integral manner. In particular, for an athermal good solvent ($\epsilon > 0$, $\epsilon_{HH} = \epsilon_{HP} = \epsilon_{PP} = 0$) we have $v_{\alpha\beta} = {}^1/_4$ and $v = 1$, by definition. Thus, this state is considered as a reference state. When $\epsilon = \epsilon_{HH} = \epsilon_{HP} = \epsilon_{PP} = 0$, we deal with a phantom chain for which $v_{\alpha\beta} = 0$ and $v = 0$ are assumed. Negative values of v correspond to a poor solvent, and v decreases as temperature is reduced. In reality, when the temperature is fixed, the change in v can be due to varying the solvent composition.

Explicitly, no solvent particles are included in the simulations; that is, the solvent is represented by a dielectric continuum. To simulate solvation effects and the time evolution of the solution in contact with a heat bath of temperature T, we augment the equations of motion by the Langevin uncorrelated noise term $\mathbf{R}_i$ which is connected with the viscosity of the solvent Γ through the fluctuation−dissipation theorem, $\langle R_{\alpha i}(0) R_{\alpha i}(t)\rangle = 2\Gamma_i k_BT\delta(t)$ ($\alpha = x, y, z$; $i = 1, 2, ..., 2N$; T is the reference temperature), and ensures that the temperature is kept constant.[14] We take the parameter Γ to be dependent on solvent-accessible surface areas (SASA). To find the values of SASA for a given configuration, we perform an analytical computation of the surface areas A_i for each specified bead.[21,22] Having A_i, one can define Γ_i as $\Gamma_i = \Gamma_0 A_i/A_{max}$, where A_{max} is the maximum solvent-accessible surface area of a bead for the model under study and the reference value of Γ_0 is taken to be equal to unity. The weighting factor A_i/A_{max} represents the degree of exposure of the bead i to the solvent. When the value of SASA for a given chain bead is zero, the frictional and random forces are zero and the Langevin equation reduces to Newton's equation of motion. For the chain in a globular conformation, this typically happens when the monomer is located in the core of a globule. On the contrary, a monomer located at the globular surface is strongly solvated; it means that A_i should be close to A_{max}, and as a result, the value of Γ_i is close to its reference value Γ_0.

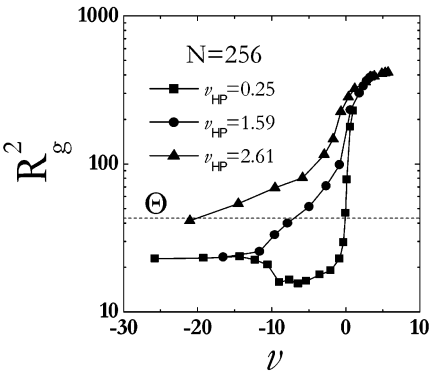

Figure 2. Mean-square radius of gyration R_g^2 as a function of solvent quality, v, at three different values of v_{HP} (0.25, 1.59, and 2.61) for the chain of length $N = 256$. The value of $R_{g\Theta}^2$ for a unperturbed chain of the same length, calculated at $\epsilon = \epsilon_{HH} = \epsilon_{HP} = \epsilon_{PP} = 0$ in eqs 1 and 2, is shown by the dashed line.

The equations of motion in conjunction with the constraints of fixed bond lengths are solved iteratively using a Newtonian iteration procedure[14,15] with the time step $\Delta t = 0.01\sigma\sqrt{m/\epsilon}$, where $m = 1$ is the mass of chain bead. For more details on the integration algorithm used in this study and the bond-constraint method, we refer to our previous publications.[11,23] In the following, the reference temperature is fixed at $T = \epsilon/k_B$, and the values of ϵ_{HH} and ϵ_{HP} (or v_{HH} and v_{HP}) are considered as only variable parameters ($\epsilon_{PP} = 0$ and $v_{PP} = {}^1/_4$). The energy parameter ϵ_{HH} responsible for hydrophobic attraction is varied in the range from −5 to 0 and the parameter ϵ_{HP} from 0 to 2. We simulate a range of chain lengths up to $N = 1024$ (2048 beads). The initial system is equilibrated for about 2×10^6 time steps, and then the production runs are performed. Typically, each production run is from 2×10^6 to 10^7 time steps, depending on the chain length N and the value of energy parameters.

Results

A gross measure of the size of the macromolecule is given by its mean-square radius of gyration, R_g^2. To obtain statistically meaningful estimates of this quantity, the system was run for times much longer than the time scale of the fluctuations in R_g^2, which increases rapidly with increasing chain length.

Figure 2 shows R_g^2 as a function of solvent quality v for a few different v_{HP} for chains of length $N = 256$. In a good solvent ($v > 0$), all the curves start at approximately the same R_g^2, but they quickly diverge from each other when solvent becomes poor ($v < 0$). Generally, the trend seen in Figure 2 is very clear: there is a consistent decrease in R_g^2 with decreasing v at all values of v_{HP} which characterize the repulsion between H and P beads. As the repulsion weakens, the decrease occurs more rapidly in the region $v \gtrsim -10$; that is, the chain self-folding or collapse occurs more easily (i.e., at larger values of v) with worsening solvent quality. In this region, the curves are sigmoidal in shape and tend to level off to a constant value at small v. This behavior is reminiscent of the usual collapse transition seen in

polymer systems when the temperature is varied.[12,13] The controlling parameter that governs the transition in the present case, v, is analogous to temperature. From the data presented in Figure 2, we can conclude that at strong H−P segregation ($v_{HP} > 1/4$) the transition region is very wide and becomes wider with increasing the v_{HP} value.

To show that the polymer undergoes a true collapse transition, we calculated the mean-square radius of gyration, $R_{g\Theta}^2$, for a phantom (unperturbed) chain of the same length (in this case, we set $\epsilon = \epsilon_{HH} = \epsilon_{HP} = \epsilon_{PP} = 0$ in eqs 1 and 2). The result is presented in Figure 2 by dashed line. It is seen that at sufficiently small v the chain size indeed becomes smaller than $R_{g\Theta}^2$, and the Θ point, where $R_g^2 = R_{g\Theta}^2$, shifts toward smaller v with increasing v_{HP}, i.e., with strengthening the H−P repulsion.

All the results presented above are somewhat expected and correspond to a general concept of the collapse transition.[12,13] However, there is some unexpected phenomenon. The inspection of the data obtained at $v_{HP} = 1/4$ ($\epsilon_{HP} = 0$) in the region $v \lesssim -10$ reveals that the HP polymer, being in a dense collapsed state, demonstrates a slow increase in R_g^2 with decreasing v, i.e., when the hydrophilic groups experience an athermal good solvent while the solvent quality for the hydrophobic groups becomes poorer. In other words, we observe an expansion of the compact conformation under poor solvent conditions. Starting from $R_g^2 = 228$ at $v = 1$, the radius of gyration rapidly drops by about 90% to reach $R_g^2 = 15.5$ at $v = -6.42$. Well below the collapse transition, R_g^2 stays approximately constant for a while and then grows again and reaches $R_g^2 = 22.8$ at the lowest value of v studied (see Figure 2). The growth of the gyration radius is rather surprising since, obviously, one would expect a chain to shrink upon the progressive worsening of solvent quality, not to expand. We will see that this phenomenon is due to polymorphic conformational transitions connected with changes in polymer shape.

Insight into the average shape of a polymer can be gained by computing the principal moments of the inertia tensor and the corresponding principal moments R_i^2 of the squared radius of gyration along the principal axes **1**, **2**, and **3** of the polymer.[24,25] The dimensionless ratios $f_1 = R_1^2/R_g^2$, $f_2 = R_2^2/R_g^2$, and $f_3 = R_3^2/R_g^2$ ($f_1 \le f_2 \le f_3$) called shape factors are used to characterize the average shape of a macromolecule.[24] For a spherical object, one has $f_1 = f_2 = f_3 = 1/3$; for a disklike object, $f_2 \approx f_3 \gg f_1$; and for a cylindrical object, $f_3 \gg f_1 \approx f_2$. For given values of v, v_{HP}, and N, after equilibration, we have computed the above-mentioned quantities of our interest.

Figure 3 presents the shape factors f_1, f_2, and f_3 of a 256-unit chain as a function of v at two different v_{HP}. It is seen that in a good solvent ($v > 0$) the average shape of the swollen chain weakly depends on v_{HP} and corresponds to a three-axes ellipsoid, the result well-known for coillike chains.[24,25] A decrease in v is accompanied by well-pronounced variations in the shape of the polymer chain. At weak H−P segregation ($v_{HP} = 1/4$), its shape asymmetry initially decreases. As the solvent quality gets worse and the chain size decreases, we find a narrow region in which the formation of disklike conformations can be observed. In yet poorer solvents, a transition into an elongated conformation with nearly cylindrical symmetry is seen (Figure 3a). This anisotropically shaped conformation turns out to be quite stable even in a very poor solvent. When the H−P segregation is stronger, the chain does not form the disklike conformations under folding (Figure 3b). In this case, the shape variation monitored during the self-folding is represented as a smooth transition from elongated ellipsoid to a stretched cylindrical object, whose shape can then become more asymmetric with decreasing v.

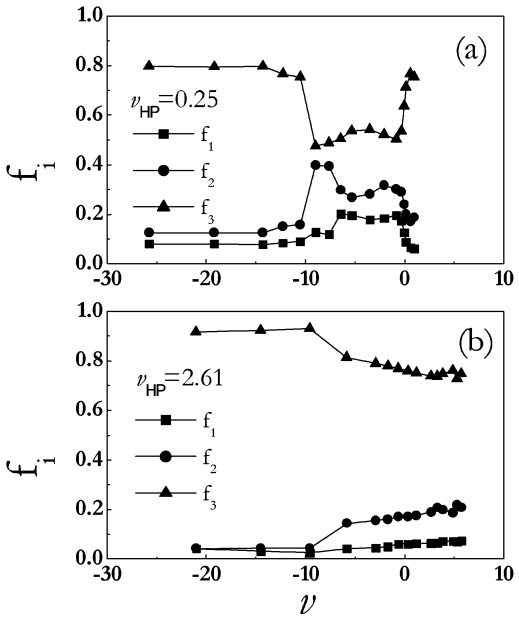

Figure 3. Shape factors f_1, f_2, and f_3 of a 256-unit chain as a function of the quality of the solvent, v, at two different values of v_{HP}: (a) $v_{HP} = 1/4$ and (b) $v_{HP} = 2.61$.

To collect information on the qualitative features of the conformations of the simulated polymers, we have directly looked at many snapshots of the system at various parameters. For a fixed $N = 256$, a series of typical snapshots obtained for a few different v and the strong H−P segregation ($v_{HP} = 2.61$) are shown in Figure 4. As expected, when the v value is close to zero, so that the repulsive interactions between monomers dominate, the chain has a usual coillike conformation (Figure 4a,b). As the solvent becomes poorer, for intermediate values of v (e.g., in the range from ≈ -2.5 to ≈ -6.0), we observe chain folding, and this leads to the formation of specific necklace-like conformations where single "pearls" of hydrophobic groups surrounded by hydrophilic groups are connected by stretched chain sections (Figure 4c,d). In this regime, the mobility of each monomer is quite high and monomer position fluctuations are still large. Pearls are locally in equilibrium, linked to one another by fluctuating chain sections. It was found that with decreasing v the size of pearls increases and, as a result, their number decreases. Finally, when $v \lesssim -8$, the pearls coalesce and form an object that looks like a sausage, which then transforms to a cylindrical-shaped object with cross section increasing very slowly as the H−H attraction grows (Figure 4e,f). Such strongly nonspherical aggregates, whose state is liquidlike, are thermodynamically stable under conditions considered. Upon visual inspection of these aggregates, we find that the hydrophobic chain finds itself in an irregularly folded (crumpled) state.

Thus, the progressive worsening of solvent quality results in the following succession of the conformational

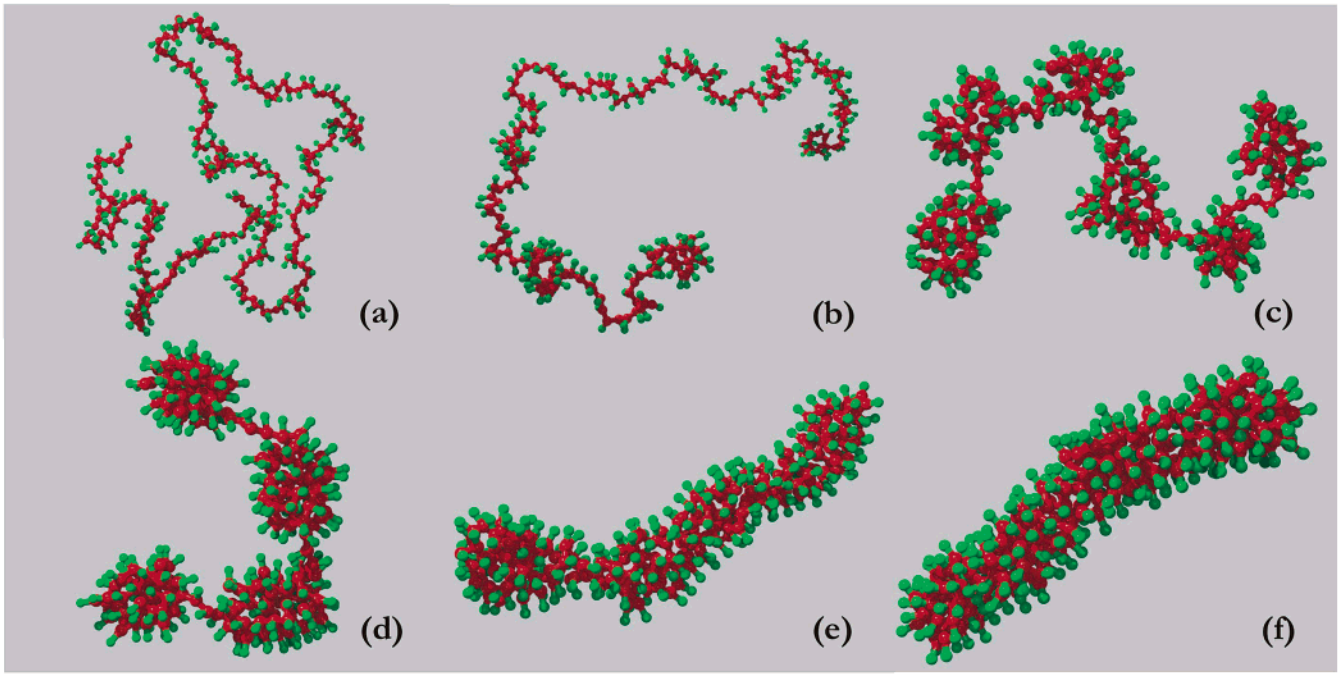

Figure 4. Snapshot pictures illustrating typical conformations of the chain of length $N = 256$ for the strong H−P segregation ($v_{HP} = 2.61$) at different values of v: (a) $v = 1.20$, (b) $v = -1.69$, (c) $v = -2.90$, (d) $v = -5.81$, (e) $v = -9.57$, and (f) $v = -14.5$. Hydrophobic beads are shown as red spheres, and hydrophilic beads are presented as green spheres. The sizes of all the spheres are schematic rather then space filling.

transitions at sufficiently strong H−P segregation: swollen coil → stretched necklace-like conformation → sausage-like object → cylindrical-shaped conformation. In principle, these qualitative observations can explain some data presented in Figure 3. We would like to emphasize that such transitions should be considered rather as a smooth shape evolution of the model HP polymer than sharp transitions. Indeed, from Figure 2 we have seen that the chain size as a function of solvent quality shows fairly smooth changes after the region where the self-folding or collapse took place. In other words, there is no well-defined temperature transition between different regimes but rather a smooth transition from the necklace-like regime to the sausage regime and further to the cylindrical regime. Therefore, it is possible to observe, e.g., a coexistence of pearls and sausage for a given solvent condition.

To gain further insight into the problem discussed, we have monitored the variation of R_g^2 at a fixed (strong) hydrophobic attraction ($v_{HH} = -15.0$) and different values of v_{HP} characterizing the H−P repulsion. The simulation results are shown in Figure 5 as a function of v for $N = 256$. In this case, the total value of v decreases due to a decrease in v_{HP}. It is seen that, in this regime, the chain can be both in swollen and in folded state, and the chain dimensions are slowly reduced when the H−P segregation weakens. The analysis of shape factors (not shown) indicates that the initially featureless coil develops a hierarchy of intramolecular self-organization: the chain conformation smoothly changes from necklace-like structure to sausage-like state and then to cylindrical state as the solvent becomes poorer and R_g^2 decreases.

As mentioned in the Introduction, for a homopolymer chain in the scaling regime (at $N \gg 1$), it is known that $R_g^2 \propto N^{2\nu}$, where ν depends on the solvent conditions ($\nu \approx 0.59$ for a swollen chain and $\nu = 1/3$ for a collapsed chain).[12] However, taking into account the results

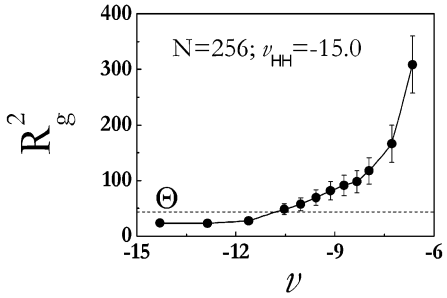

Figure 5. Mean-square radius of gyration R_g^2 of a 256-unit chain as a function of the quality of the solvent, v, at a fixed strength of hydrophobic interaction ($v_{HH} = -15.0$). The dashed line shows the value of $R_{g\Theta}^2$ for a phantom chain of the same length.

discussed above, we can expect that the behavior of elongated cylindrical-shaped aggregates observed for our HP model in a poor solvent should be different. To verify this hypothesis, we have calculated the values R_g^2 and f_i for a few different N at sufficiently strong attraction between H beads ($v_{HH} = -15.0$). Figure 6 shows R_g^2 and f_i as a function of N for two different values of v_{HP}. Also, in Figure 6a we present the mean-square radius of gyrations, $R_{g\Theta}^2$, found for phantom chains. As expected, $R_{g\Theta}^2$ scales with N as $R_{g\Theta}^2 \propto N$ for all the chain lengths considered, starting at $N = 32$. On the other hand, for the HP polymer with intrachain nonbonded interactions, the power law $R_g^2 \propto N^{2\nu}$ starts only after $N \approx 196$ (for $v_{HP} = 1/4$) and $N \approx 32$ (for $v_{HP} = 2.61$), and a fit to the last points yields a scaling exponent of $2\nu = 1.74 \pm 0.07$ (for $v_{HP} = 1/4$) and $2\nu = 1.80 \pm 0.05$ (for $v_{HP} = 2.61$), somewhat less than the value corresponding to a rigid-rod-like object with $2\nu = 2$. Also, from Figure 6b we can see that the average shape of the chain is close to spherical at small N and becomes more elongated and gradually approaches the shape of a perfect cylindrical body with increasing N.

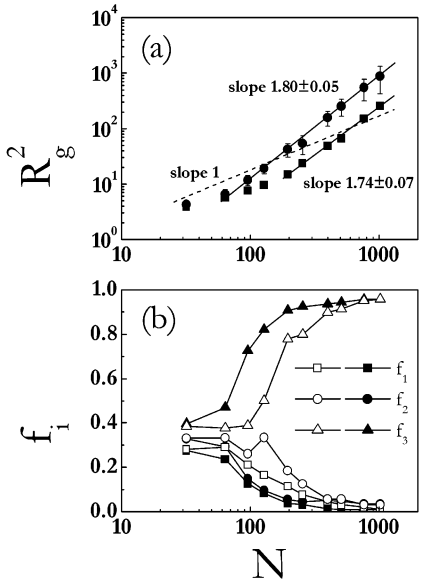

Figure 6. (a) Mean-square radius of gyration as a function of the chain length N in a solvent of poor quality ($v_{HH} = -15.0$), at (■) $v_{HP} = 1/4$ and (●) $v_{HP} = 2.61$. (b) Shape factors f_1, f_2, and f_3 for the same solvent conditions, at $v_{HP} = 1/4$ (open symbols) and $v_{HP} = 2.61$ (closed symbols). (a) Dashed line shows the value of $R_{g\Theta}^2$ as a function of N for a phantom chain.

This is consistent with the results of Figure 4 at small v.

Discussion

Let us now try to rationalize some results of the computer simulation described above, using simple theoretical arguments of refs 26−28. Our starting point will be based on the fact that, for the model considered, each of the hydrophobic (hydrophilic) groups has a tendency to have hydrophobic (hydrophilic) nearest neighbors and to avoid having hydrophilic (hydrophobic) nearest neighbors in a poor solvent. It is clear that such a situation is very similar to that characteristic of usual low-molecular-weight amphiphiles, which form micelles in a dilute solution. Indeed, our extended HP model (Figure 1d) bears resemblance to a system of N small chemically connected HP surfactants. In a polar solvent, surfactants can form micelles with dense hydrophobic core surrounded by hydrophilic shell. At fixed thermodynamic conditions, the average size of the micellar core remains in principle constant and depends only on the number of particles in the aggregate, N. If the aggregation number N is not too large ($N \lesssim 10^2$), the shape of the aggregate varies rather weakly with N and does not deviate significantly from spherical one. However, as shown theoretically[28] and in computer simulations[27] for the strong segregation regime (in the context of phase separation phenomena[19]), various polymorphic transitions are possible when N becomes sufficiently large. The equilibrium size and shape of a hydrophobic aggregate is determined by a balance between the interfacial free energy, F_S, and the core free energy, F_H.[28] Obviously, the minimum of F_S corresponds to an aggregate of spherical shape. However, because of connection between H and P groups, a large spherical aggregate is geometrically impossible without "structural defects", i.e., the inclusions of hydrophilic P groups inside the hydrophobic core. The presence of such defects leads to an increase in F_H. As result of the competition between F_S and F_H, the minimum of the total free energy is attained for nonspherical core geometries, when each hydrophobic group is close to core surface, while all the hydrophilic groups are positioned outside the hydrophobic core. In particular, the increase of N can stimulate a polymorphic transition from a near-spherical micellar core, whose molecular organization is dominated by surface effects, toward disklike or elongated striplike aggregates stabilized by a more uniform compact packing of the hydrophobic groups as well as by pushing away the hydrophilic groups from the core.[27,28] Of course, a large micelle can disintegrate and form splinters of smaller size, but this process is not possible for "chemically connected surfactants" composing the HP chain simulated in this study. That is why we observe the stretched conformations for sufficiently long HP chains at strong hydrophobic attraction (see Figures 2−4). Note also that the interfacial free energy should be proportional to r_c^3, where r_c is the cutoff distance in the potential $u_s(r)$, eq 2, whereas the free energy of hydrophobic core is proportional to r_c^2.[28] Therefore, for large r_c, the surface term must dominate, thus stabilizing a spherical shape of micellar core. For small r_c, the behavior should be opposite, so that we expect a transition from the spherical to nonspherical geometry upon decreasing r_c. In general, this situation corresponds to that realized in the present study where site−site interactions are of short-range ($r_c = 4\sigma$). Following the theoretical predictions,[28] the instabilities of spherical aggregate shape are more pronounced when the incompatibility of H and P species is increased. This conclusion is consistent with our results. Indeed, we have found that the stronger the H−P repulsion is, the more stretched the folded HP chain is, as shown by the data presented in Figures 2 and 4−6.

We would like to emphasize once more that the physical picture observed in our simulations is generally very close to that known for processes of micellization in dilute solutions of surfactants.[29,30] In fact, the introduced side-chain HP model displays a behavior that is rather common for polysoaps which, due to their amphiphilic character, are able to build up self-assembled structures in polar as well as in apolar media.[31−33] From this viewpoint, an important issue was to evaluate how the balance between the attractive forces stabilizing the hydrophobic aggregates and the repulsive short-range interactions of polar groups affects intrachain self-organization. Following this line, we should treat the conformational transitions found for the extended HP model rather as an intrachain micellization than as a true coil-to-globule transition leading to the $R_g \propto N^{1/3}$ scaling.[12] In particular, the necklace-like conformation with hydrophobic pearls surrounded by hydrophilic groups (Figure 4c,d) has to be considered as a string of micelles, but it has nothing common with the pearl-necklace model structure proposed by Rubinstein and co-workers[34−37] for flexible polyelectrolytes in poor solvents where, due to the Rayleigh charge instability, highly stretched segments alternate with collapsed (micro)globules along the chain. Structurally, the intramolecular micelles observed for the necklace-like state are similar to micelles formed by free low-molecular-weight surfactants; however, unlike ordinary micelles, intramolecular micelles need no critical concentration of polysurfactants for their formation because in this case there is no loss of translational entropy.

On the other hand, the conformational transitions observed in our simulations resemble in some aspects

the so-called zipping transitions,[38] the process in which two strongly attracting strands composing the polymer come in contact in such a way as to form a bound double structure, which remains swollen and does not assume compact configurations. The simulations carried out in ref 38 for a two-dimensional model have shown that, depending on the values of the energy parameters in the model, there is either a first-order collapse from a swollen phase to a compact phase of spiral type or a continuous transition to an intermediate zipped phase followed by a first-order collapse at lower temperatures. Our cylindrical-shaped conformations in which the hydrophobic backbone is in a locally collapsed state (Figure 4e,f) look a lot like three-dimensional zipped structures. Also, from a formal point of view, these conformations are similar to the earlier cylindrical model of polyelectrolytes in a poor solvent.[39,40]

The behavior of the cylindrical-shaped structures as a function of chain length shown in Figure 6a is of great interest. The fact that the scaling exponent found here is slightly smaller than the rodlike prediction of $\nu = 1$ is likely due to the fact that N is very close to, though not yet in, the scaling regime. Nevertheless, it is believed that in the $N \rightarrow \infty$ limit, because of strong thermal fluctuations, the locally folded chain as a whole would look like an infinite coiled hose (or a wormlike superchain) having a finite thickness and a finite persistent length, and the limiting scaling exponent would be close to that expected for the good solvent regime, due to repulsive interactions between outer hydrophilic groups shielding hydrophobic core in the resulting core−shell structure. In other words, for very large N we expect a crossover from the $R_g \propto N$ regime to the $R_g \propto N^{0.59}$ regime. Of course, the issue of the behavior in the $N \rightarrow \infty$ limit is still open, and further discussion is needed. Another open question is the structure of the ground state in the low-temperature limit, but this is beyond the scope of the present paper. The next open issue is the effect of disorder on the conformational transitions, which would allow one to understand the behavior of models of hydrophobic−amphiphilic or hydrophilic−amphiphilic copolymers more relevant for applications to chemistry or biology than the simple regular HP model simulated here. In this connection one can also mention the problem of interchain aggregation in solutions. All these problems will be discussed in our forthcoming publications.

Finally, we may add a few words about experimental evidences of some facts predicted in the present simulations. Experimentally, intramolecular nonspherical aggregates have been observed for solutions of polymeric amphiphiles in the large number of works (see, e.g., refs 41−44). In particular, cylindrical-shaped,[41,43,44] ellipsoidal-shaped,[41] and disk-shaped[44] microstructures have been reported. The strongly extended conformations with cylindrical symmetries are characteristic of giant hydrophobic/hydrophilic Janus micelles in selective solvents.[45,46] A variety of intramolecular nonspherical microstructures are observed for amphiphilic graft copolymers. It is well-documented that in a selective solvent, which is poor for backbone and good for side groups, flexible graft copolymers can undergo collapse transition into unimolecular micelle-like structures in which the collapsed backbone is covered with side groups.[47] Kikuchi and Nose,[48] in their studies of poly(methyl methacrylate)-*graft*-polystyrene with short branches in mixed selective solvents, have observed the formation of a thermodynamically stable single-chain multimicellar microstructures. Their results revealed that the microstructures are quite rigid and on average consist of approximately five flowerlike micelles on each copolymer chain, resembling a string of closely packed pearls. The size of these microstructures cannot be explained using the models of a flexible string of flowerlike micelles[32] or a collapsed chain of micelles[49] but can be explained when the chain conformation is considered as a stretched sequence of a few linearly connected intramolecular micelles.[48] Also, it was found that the number of micelles per chain decreases with decrease of temperature.[48] If solvent quality for the polymer backbone changes from nearly Θ condition to strongly nonsolvent quality, keeping solvent quality for the side chains good, a unimolecular micelle of wormlike chain appears, followed by a cylindrical unimolecular micelle, where the backbone is stabilized by soluble side groups.[48] Generally, the same trends are observed for the side-chain HP model simulated in our work. Very recently, Kiriy et al.[50] have studied solvent-induced aggregation of poly(3-alkylthiophene)'s (PATs) by means of AFM and UV−vis spectroscopy. In a selective solvent, which is a poor solvent for polythiophene backbone but a good solvent for alkyl side groups, PAT molecules fold back on themselves and form wormlike nanostructures on the single-molecule level.[50] This state maximizes unfavorable interactions between the poorly soluble backbone and solvent. Our results are consistent with these experimental observations.

The perhaps most interesting observation following from our calculation is the irregular behavior of the mean-square radius of gyration seen in Figure 2 at $\nu_{HP} = {}^1/_4$. In the literature, one can find some experimental data confirming this result. In a series of papers,[51,52] Nakata and Nakagawa have studied the coil−globule transition by static light scattering measurements on poly(methyl methacrylate) in a selective solvent. They have found that the chain expansion factor, $\alpha^2 = R_g^2/R_{g\Theta}^2$, plotted against the reduced temperature, $\tau = 1 - \Theta/T$, first decreases with decreasing τ, as it should be, but then begins to increase (see, e.g., Figure 2 presented in ref 52). In the authors opinion,[52] "the increase of α^2 with decreasing temperature conflicts with theoretical predictions and an intuitive notion of the expansion factor." However, taking into account the amphiphilic nature (although weakly pronounced) of poly(methyl methacrylate) and the simulation data reported here for the extended HP model, this "anomalous" behavior can be understood. Indeed, in solvent selective to side groups, the incompatibility of chemically different groups is effectively increased when the attraction between groups composing the chain backbone becomes stronger. This is accompanied by pushing away the soluble side groups from the insoluble micellar core and by stretching the macromolecule as a whole, the behavior observed in Figure 2a.

Very recently, Williams and co-workers[53] have studied the structural changes and chain conformations of a series of hydrophobic sodium poly(styrene-*co*-styrenesulfonate)'s of various charge fractions in a poor solvent using static light scattering and small-angle X-ray scattering techniques. By varying the charged monomer fraction, f, it was possible to change the degree of hydrophobity of this copolymer and the corresponding hydrophobic/hydrophilic interactions. From the scattering measurements, the so-called apparent radii of

gyration, R_g^{app}, were determined for different values of f and concentrations. From the analysis of these results (see Tables 1 and 2 of ref 53) it is seen that the values of R_g^{app} show an irregular behavior as a function of f at all the polymer concentrations studied. At large f, when the repulsive electrostatic forces dominate, the copolymer chains have an expanded conformation. With decreasing f, the intrachain short-range hydrophobic attractions begin to dominate, and as a result, the chain size decreases. However, at $f \lesssim 1/2$, an unexpected increase in R_g^{app} is distinctly observed; although, at first sight, R_g^{app} should further decrease, taking into account a monotonic growth in hydrophobic attraction. It is clear that such an "unexpected" behavior is consistent with our simulations and can be explained on the basis of the discussion presented above.

Conclusion

In this paper we have developed an extended "two-letter" hydrophobic/hydrophilic model (called the side-chain HP model) to simulate amphiphilic homopolymers. In contrast to the standard "beads-on-a-string" HP model,[1,2] our model incorporates the dualistic nature of monomer units, each consisting of hydrophobic and hydrophilic species. Using this model, we have reported on the results of extensive molecular dynamics simulations of the hydrophobically driven conformational transitions under the variation of solvent conditions. The main question concerning the single chain, intramolecular self-assembly was addressed: What is the effect of the intrachain aggregation on the equilibrium conformation of polymeric amphiphiles? We have found that for the side-chain HP model a variety of novel structures are possible in a poor solvent, depending on the interaction between hydrophobic (H) and hydrophilic (P) sites. In particular, the thermodynamically stable anisometric structures have been observed, including disklike structures, stretched necklace-like conformations, sausage-like objects, and cylindrical-shaped conformations. All these microstructures are formed due to intramolecular segregation of chemically different H and P groups: the internal arrangement of the monomers within these microstructures obviously tends to minimize the number of H−P contacts unfavorable under given solvent conditions. Of course, the separation of H and P groups cannot be as perfectly realized due to the chain connectivity constraints, thus producing micelle-like core−shell aggregates. Also, we have demonstrated that the chain size R_g as a function of the quality of the solvent can behave in an irregular manner, showing an increase when the solvent becomes poorer for hydrophobic sites. This unusual behavior is connected with the formation of strongly elongated core−shell conformations having a locally cylindrical symmetry and consistent with existing experimental data.[52,53] Moreover, for the range of the chain lengths N simulated in the present study ($N \leq 1024$), the formation of such conformations can lead to the $R_g \propto N^{0.9}$ scaling under a poor solvent condition.

Acknowledgment. The authors acknowledge useful discussions with Igor Potemkin and Ivan Okhapkin. The financial support from the Alexander-von-Humboldt Foundation, Program for Investment in the Future (ZIP), INTAS (project # 01-607), and Russian Foundation for Basic Research is highly appreciated.

References and Notes

(1) Lau, K. F.; Dill, K. A. *Macromolecules* **1989**, *22*, 3986.
(2) Lau, K. F.; Dill, K. A. *Proc. Natl. Acad. Sci. U.S.A.* **1990**, *87*, 6388.
(3) Honeycutt, J. D.; Thirumalai, D. *Biopolymers* **1992**, *32*, 695.
(4) Shakhnovich, E. I.; Gutin, A. M. *Proc. Natl. Acad. Sci. U.S.A.* **1993**, *90*, 7195.
(5) Pande, V. S.; Grosberg, A. Yu.; Tanaka, T. *Proc. Natl. Acad. Sci. U.S.A.* **1994**, *91*, 12972.
(6) Dokholyan, N. V.; Buldyrev, S. V.; Stanley, H. E.; Shakhnovich, E. I. *Fold. Des.* **1998**, *3*, 577.
(7) Irbäck, A.; Peterson, C.; Potthast, F.; Sandelin, E. *Phys. Rev. E* **1998**, *58*, R5249; *Structure* **1999**, *7*, 347. Irbäck, A.; Sandelin, E. *J. Chem. Phys.* **1999**, *110*, 12256.
(8) Giugliarelli, G.; Micheletti, C.; Banavar, J. R.; Maritan, A. *J. Chem. Phys.* **2000**, *113*, 5072.
(9) Soddemann, T.; Dünweg, B.; Kremer, K. *Eur. Phys. J. E* **2001**, *6*, 409.
(10) Pande, V. S.; Grosberg, A. Yu.; Tanaka, T. *Rev. Mod. Phys.* **2000**, *72*, 259.
(11) Khalatur, P. G.; Novikov, V. V.; Khokhlov, A. R. *Phys. Rev. E* **2003**, *67*, 051901.
(12) Lifshitz, I. M.; Grosberg, A. Yu.; Khokhlov, A. R. *Rev. Mod. Phys.* **1978**, *50*, 683. Grosberg, A. Yu.; Kuznetsov, D. V. *Macromolecules* **1992**, *25*, 1970.
(13) Grosberg, A. Yu.; Khokhlov, A. R. *Statistical Physics of Macromolecules*; American Institute of Physics: New York, 1994.
(14) Allen, M. P.; Tildesley, D. J. *Computer Simulation of Liquids*; Claredon Press: Oxford, 1990.
(15) Andersen, H. C. *J. Comput. Phys.* **1983**, *52*, 24.
(16) Tanford, C. *The Hydrophobic Effect: Formation of Micelles and Biological Membranes*; John Wiley & Sons: New York, 1973.
(17) Hummer, G.; Garde, S.; Garcia, A. E.; Paulaitis, M. E.; Pratt, L. R. *J. Phys. Chem. B* **1998**, *102*, 10469.
(18) Huang, D. M.; Chandler, D. *Proc. Natl. Acad. Sci. U.S.A.* **2000**, *97*, 8324.
(19) Bates, F. S.; Fredrickson, G. H. *Annu. Rev. Phys. Chem.* **1996**, *41*, 525.
(20) Nyrkova, I. A.; Khokhlov, A. R.; Doi, M. *Macromolecules* **1993**, *26*, 3601.
(21) Wesson, L.; Eisenberg, D. *Protein Sci.* **1992**, *1*, 227.
(22) Augspurger, J. D.; Scheraga, H. A. *J. Comput. Chem.* **1996**, *17*, 1549.
(23) Khalatur, P. G.; Khokhlov, A. R.; Mologin, D. A.; Reineker, P. *J. Chem. Phys.* **2003**, *119*, 1232.
(24) Solc, K.; Stockmayer, W. H. *J. Chem. Phys.* **1971**, *54*, 2756.
(25) Khalatur, P. G.; Khokhlov, A. R.; Mologin, D. A.; Zheligovskaya, E. A. *Macromol. Theory Simul.* **1998**, *7*, 299.
(26) Eriksson, J. C.; Ljunggren, S. *Langmuir* **1990**, *6*, 895.
(27) Khalatur, P. G.; Khokhlov, A. R.; Nyrkova, I. A.; Semenov, A. N. *Macromol. Theory Simul.* **1996**, *5*, 713.
(28) Khalatur, P. G.; Khokhlov, A. R.; Nyrkova, I. A.; Semenov, A. N. *Macromol. Theory Simul.* **1996**, *5*, 749.
(29) *Micellization, Solubilization, and Microemulsions*; Mittal, K. L., Ed.; Plenum Press: New York, 1977; Vol. 1 and 2.
(30) Smit, B. Computer Simulations of Surfactants. In *Computer Simulation in Chemical Physics*; Allen, M. P., Tildesley, D. J., Eds.; Kluwer Academic Publishers: Dordrecht, 1993; pp 461−472.
(31) Laschewsky, A. *Adv. Polym. Sci.* **1995**, *124*, 1 and references cited therein.
(32) Borisov, O. V.; Halperin, A. *Langmuir* **1995**, *11*, 2911. Borisov, O. V.; Halperin, A. *Europhys. Lett.* **1996**, *34*, 657. Borisov, O. V.; Halperin, A. *Macromolecules* **1996**, *29*, 2612.
(33) Zhou, S. Q.; Chu, B. *Adv. Mater.* **2000**, *12*, 545.
(34) Dobrynin, A. V.; Rubinstein, M.; Obukhov, S. P. *Macromolecules* **1996**, *29*, 2974.
(35) Dobrynin, A. V.; Rubinstein, M. *Macromolecules* **1999**, *32*, 915.
(36) Dobrynin, A. V.; Rubinstein, M. *Macromolecules* **2000**, *33*, 8997.
(37) Dobrynin, A. V.; Rubinstein, M. *Macromolecules* **2001**, *34*, 1964.
(38) Baiesi, M.; Carlon, E.; Orlandini, E.; Stella, A. L. *Phys. Rev. E* **2001**, *63*, 041801.
(39) Khokhlov, A. R. *J. Phys. A.: Math. Gen.* **1980**, *13*, 979.
(40) Khokhlov, A. R.; Khachaturian, K. A. *Polymer* **1982**, *23*, 1742.
(41) Shih, L.-B.; Mauer, D. H.; Verbrugge, C. J.; Wu, C. F.; Chang, S. L.; Chen, S. H. *Macromolecules* **1988**, *21*, 3235.
(42) Schwarzwälder, C.; Meier, W. *Macromolecules* **1997**, *30*, 4601.

(43) Wataoka, I.; Urakawa, H.; Kobayashi, K.; Akaike, T.; Schmidt, M.; Kajiwara, K. *Macromolecules* **1999**, *32*, 1816.
(44) Thünemann, A. F.; Wendler, U.; Jaeger, W.; Schnablegger, H. *Langmuir* **2002**, *18*, 4500.
(45) Liu, G.; Quiao, L.; Guo, A. *Macromolecules* **1996**, *29*, 5508.
(46) Erhardt, R.; Böker, A.; Zettl, H.; Kaya, H.; Pyckhout-Hintzen, W.; Krausch, G.; Abetz, V.; Müller, A. H. E. *Macromolecules* **2001**, *34*, 1069.
(47) Sheiko, S. S.; Prokhorova, S. A.; Beers, K. L.; Matyjaszewski, K.; Potemkin, I. I.; Khokhlov, A. R.; Möller, M. *Macromolecules* **2001**, *34*, 8354.
(48) Kikuchi, A.; Nose, T. *Macromolecules* **1996**, *29*, 6770.
(49) Semenov, A. N.; Joanny, J.-P.; Khokhlov, A. R. *Macromolecules* **1995**, *28*, 1066.
(50) Kiriy, M.; Jahne, E.; Adler, H.-J.; Schneider, M.; Kiriy, A.; Gorodyska, G.; Minko, S.; Jehnichen, D.; Simon, P.; Fokin, A. A.; Stamm, M. *Nano Lett.* **2003**, *3*, 707.
(51) Nakata, M.; Nakagawa, T. *Phys. Rev. E* **1997**, *56*, 33838.
(52) Nakata, M.; Nakagawa, T. *J. Chem. Phys.* **1999**, *110*, 2703.
(53) Carbajal-Tinoko, M. D.; Ober, R.; Dolbnya, I.; Bras, W.; Williams, C. E. *J. Phys. Chem. B* **2002**, *106*, 12165.

MA0350563